V European Conference on Computational Fluid Dynamics
ECCOMAS CFD 2010
J. C. F. Pereira and A. Sequeira (Eds)
Lisbon, Portugal,14-17 June 2010

IS THE DYNAMIC PROCEDURE APPROPRIATE FOR ALL SGS MODELS ?

H. Baya Toda*, Karine Truffin* and Franck Nicoud†

*Institut Français du Petrole,
1-4 Avenue Bois preau 92852 Rueil-Malmaison
e-mail: hubert.baya-toda@ifp.fr
†I3M CNRS-Universite Montpellier 2
address
e-mail: franck.nicoud@univ-montp2.fr, karine.truffin@ifp.fr

Key words: Large eddy simulation, Germano-identity, Wall-bounded flows, Subgrid-scale model

Abstract. *The rapid growth of supercomputers will probably make the use of Large eddy simulations (LES) more accessible for industrial applications in a near future. It is then important to develop accurate models able to represent as well as possible the turbulence effects in very complex and wall-bounded flows. While the Smagorinsky model is known for its extradissipation in near wall regions, other models with the appropriate near wall behaviour are now available (e.g. WALE and Vreman model). Still, values of the constants proposed by the authors are expected to be not universal notably in complex geometries.*
In this study, a dynamic version of the WALE subgrid model has been developped based on the Germano-identity. The dynamic WALE, the dynamic Smagorinsky and the WALE models are first tested on the homogeneous isotropic turbulent (HIT) experiment of Comte-Bellot and Corsin (CBC). Large eddy simulations of an isothermal turbulent channel flow are then performed and results are compared with the DNS of Moser et al. at wall Reynolds number Re_τ 395 and 590. This last test illustrates how the dynamic procedure combined with the WALE fails to correctly model the mean velocity. It leads to very high values of the WALE constant near the wall and to an over prediction of the turbulent viscosity in the buffer-layer. It is then shown in the paper that the dynamic procedure might degrade any SGS model with the proper wall behaviour. Finally, a cure to this problem is proposed and used to built an appropriate dynamic WALE model which proves accurate in the channel flow and promising in an industrial like configuration.

1 INTRODUCTION

One of the most challenging aspect of LES modelling is certainly near wall effects. For industrial applications the knowledge of the latter is important for the optimisation of the energy consumption (heating or cooling); it is then necessary to develop accurate LES models able to represent as well as possible wall effects.
Since the Smagorinsky model[1], many attempts have been done to meet the requirements of modelling in presence of a solid wall. These requirements[2] are the y^3 asymptotic behaviour and the capability to represent laminar-to-turbulent transition. To this respect, the use of damping function[3] or of the Germano-identity[4] to dynamically adapt the model constant have been successfully used. This approach is most referred in the literature as an optimisation method and is more suitable for complex geometries where the knowledge of the distance to the wall is not straightforward. More recently the WALE model developed by Nicoud and Ducros[5] and the Vreman's[6] model have allowed to respect these requirements without using any damping functions or dynamic procedure. Still the value of the constant proposed by the authors is expected to vary depending on the flow and the geometry.
The present paper is organized as follows: in section 2, the governing equations and the different subgrid scales models are presented. In section 3, the models and their implementation are validated by considering the homogeneous isotropic turbulence configuration of Comte et Bellot[7]. In section 4, results by considering an isothermal turbulent channel computed with the different models are compared. The problem which arises when considering the WALE dynamic model based on the Germano-identity is also presented. A cure to the previous problem is presented in section 5 and the results with the improved dynamic WALE model are presented in the same section followed by a conclusion.

2 GOVERNING EQUATIONS AND SGS MODELS

The filtered compressible Navier-Stokes equations are solved in this study but their incompressible counterpart are presented here for simplicity since only low Mach number flows will be considered:

$$\frac{\partial \bar{u}_j}{\partial x_j} = 0 \tag{1}$$

$$\frac{\partial \bar{u}_i}{\partial t} + \frac{\partial (\bar{u}_i \bar{u}_j)}{\partial x_j} = -\frac{1}{\bar{\rho}} \frac{\partial \bar{p}}{\partial x_i} + \nu \frac{\partial^2 \bar{u}_i}{\partial x_i \partial x_j} + \frac{\partial \tau_{ij}^{sgs}}{\partial x_j} + S_i$$

where t is time, p the pressure, ρ the density, ν the kinematic viscosity, S_i a source term and τ_{ij}^{sgs} the subgrid scale (SGS) tensor expressed as:

$$\tau_{ij}^{sgs} = \bar{u}_i \bar{u}_j - \overline{u_i u_j} \tag{2}$$

An eddy viscosity approach has been chosen to model the SGS tensor which is then expressed as :

$$\tau_{ij}^{sgs} - \frac{1}{3}\tau_{kk}^{sgs}\delta_{ij} = 2\nu^{sgs}\bar{S}_{ij} \tag{3}$$

where $\bar{S}_{ij}$ is the strain rate based on the filtered velocity $\bar{u}_i$ and ν^{sgs} the eddy viscosity.

2.1 WALE model[5]:

Like the Vreman's model[6], the WALE model[5] does not generate SGS activity for pure shear flows and was built to recover the right asymptotic behaviour near solid walls and the eddy viscosity is expressed as follows:

$$\nu^{sgs} = C_w^2\bar{\Delta}^2|\bar{OP}| \tag{4}$$

where $C_w = 0.5$, $\bar{\Delta}$ is the filter size and $\bar{OP}$ an operator defined as follows:

$$|\bar{OP}| = \frac{(S_{ij}^d S_{ij}^d)^{3/2}}{(\bar{S}_{ij}\bar{S}_{ij})^{5/2} + (S_{ij}^d S_{ij}^d)^{5/4}} \tag{5}$$

where S_{ij}^d is the symmetric traceless part of the square of the strain rate, expressed as:

$$S_{ij}^d = \bar{S}_{ik}\bar{S}_{kj} + \bar{\Omega}_{ik}\bar{\Omega}_{kj} - \frac{1}{3}\delta_{ij}[\bar{S}_{mn}\bar{S}_{mn} + \bar{\Omega}_{mn}\bar{\Omega}_{mn}], \tag{6}$$

where $\bar{\Omega}_{ij}$ is the rotation rate based on the filtered velocity $\bar{u}_i$

2.2 Dynamic WALE model

To develop the dynamic WALE model, a second test filter $\hat{\Delta}$ bigger than the initial filter $\bar{\Delta}$ is first considered, the Navier-Stokes equations filtered at the test filter level are then expressed as follows:

$$\frac{\partial\hat{\bar{u}}_i}{\partial t} + \frac{\partial(\hat{\bar{u}}_i\hat{\bar{u}}_j)}{\partial x_j} = \frac{1}{\hat{\bar{\rho}}}\frac{\partial\hat{\bar{p}}}{\partial x_i} + \nu\frac{\partial^2\hat{\bar{u}}_i}{\partial x_i\partial x_j} + \frac{\partial T_{ij}^{sgs}}{\partial x_j}, \tag{7}$$

where T_{ij}^{sgs} is the sgs tensor at the test filter level. Using the Germano-identity, we have the following relationship between T_{ij}^{sgs} and τ_{ij}^{sgs} :

$$T_{ij}^{sgs} - \hat{\tau}_{ij}^{sgs} = L_{ij} \tag{8}$$

L_{ij} is the Leonard term expressed as:

$$L_{ij} = \widehat{\bar{u}_i\bar{u}_j} - \hat{\bar{u}}_i\hat{\bar{u}}_j \tag{9}$$

The WALE eddy viscosity model is used for the SGS tensors at the two level so that equation Eq.(8) becomes:

$$C_w^2 \hat{\Delta}^2 |\hat{\bar{O}P}| \hat{\bar{S}}_{ij} - (C_w^2 \widehat{\bar{\Delta}^2 |\bar{O}P|} \bar{S}_{ij}) = L_{ij} \tag{10}$$

If C_w is assumed constant over a distance at least equal to the testfilter width, its dynamic value can be expressed as follows using the least square method of Lilly[8]:

$$C_w^2 = \frac{1}{2} \frac{< L_{ij} M_{ij}^w >^+}{< M_{ij}^w M_{ij}^w >} \tag{11}$$

with

$$M_{ij}^w = \hat{\Delta}^2 |\hat{\bar{O}P}| \hat{\bar{S}}_{ij} - (\bar{\Delta}^2 \widehat{|\bar{O}P|} \bar{S}_{ij}) \tag{12}$$

The superscript + in the expression Eq.(11) denotes a positive clipping of all negative values to zero and the sign <> is a stabilisation method that consists in a local volume averaging. In contrary to what is often done for the dynamic Smagorinsky[4] model and recently for the WALE model[9], the stabilisation is not performed over homogeneous directions but locally; it is then well adapted to complex geometries.

2.3 Dynamic Smagorinsky model[4]

The dynamic Smagorinsky constant was calculated with the same consideration as for the dynamic WALE constant. The only difference is the operator $|\bar{OP}|$ in the expression of M_{ij}^s :

$$M_{ij}^s = \hat{\Delta}^2 |\hat{\bar{O}P^s}| \hat{\bar{S}}_{ij} - (\bar{\Delta}^2 \widehat{|\bar{O}P^s|} \bar{S}_{ij}) \tag{13}$$

with $|\bar{OP^s}|$ the second invariant of the strain rate based on the filtered velocity $\bar{u}_i$ expressed as :

$$|\bar{OP^s}| = \sqrt{2 \bar{S}_{ij} \bar{S}_{ij}} \tag{14}$$

and the dynamic Smagorinsky constant is expressed as :

$$C_s^2 = \frac{1}{2} \frac{< L_{ij} M_{ij}^s >^+}{< M_{ij}^s M_{ij}^s >} \tag{15}$$

The WALE[5] , the dynamic WALE and the dynamic Smagorinsky[4] models will be denoted respectively as WA, WAD and SMD.

2.4 Numerical solver

The calculations were carried out with AVBP, the CFD solver developed at CERFACS. This parallel solver offers the capability to handle unstructured and structured grids in order to solve the 3D compressible reacting Navier-Stokes equations with a cell-vertex formulation. A centered Galerkin finite element method with a three step Runge-Kutta temporal method has been used. The numerical solver is fourth order accurate in space and third order in time. The efficiency of the numerical method used and the AVBP code has already been successfully tested in the past years by Colin and Rudgyard[10], Moreau et al.[11] and recently by Cabrit and Nicoud[12].

3 HOMOGENEOUS ISOTROPIC TURBULENCE

The SGS models are first tested on the HIT experiment of Comte-Bellot and Corsin[7]. This experiment has already been widely [4,13,14,15] used either to validate purely eddy-viscosity models or to find their constant values. The characteristics of the CBC experiment are summarised in table.1.

$t* = \frac{U_o t}{M}$	$u_{rms}(cm.s^{-1})$	$\epsilon(cm^2.s^{-3})$	$\eta(cm)$	$\lambda(cm)$	R_λ
42	22.2	4740	0.029	0.484	71.6
98	12.8	633	0.048	0.764	65.3
171	8.95	174	0.066	1.02	60.7

Table 1: Characteristics of the HIT of CBC where $U_o = 10m/s$ is the convective velocity, ϵ is the kinetic energy dissipation, η is the kolmogorv scale, $M = 5.08cm$ is the grid size, λ the Taylor micro scale and R_λ the Reynolds number based on λ.

The experimental validation consists in initialising in a computation with a velocity field whose spectrum matches the first spectum at time $t^* = 42$ and comparing the experimental and the spectra at times $t^* = 98$ and $t^* = 171$. The reference length and the reference velocity are respectively $L_{ref} = \frac{L_B}{2\pi}$ and $U_{ref} = \sqrt{3/2}u_{rms}(t* = 42)$. $L_B = 11M$ is the length of the computation box. The simulations are performed over a 61^3 mesh. Since the experimental evolution of the kinetic energy is not available, the results will be compared with the data of the EQDNM simulations of Park and Mahesh[16].

Figure 1 shows the evolution of the spectra predicted by the static WALE model[5] and the dynamic WALE described in section 2.2 compared with the experiment.

The first spectrum corresponds to the initialisation at time $t^* = 42$. As expected, the spectra obtained with WALE[5] and the dynamic WALE models are very similar at the following time and in good agreement with the experiment for wavelengths smaller than $K < \frac{K_c}{2}$. In fact, for greater wavelengths the energy is under predicted. But those wavelengths are resolved with least than 4 points. The discrepancies observed are probably due to numerical errors rather than SGS model limitations. Nevertheless, the global energy

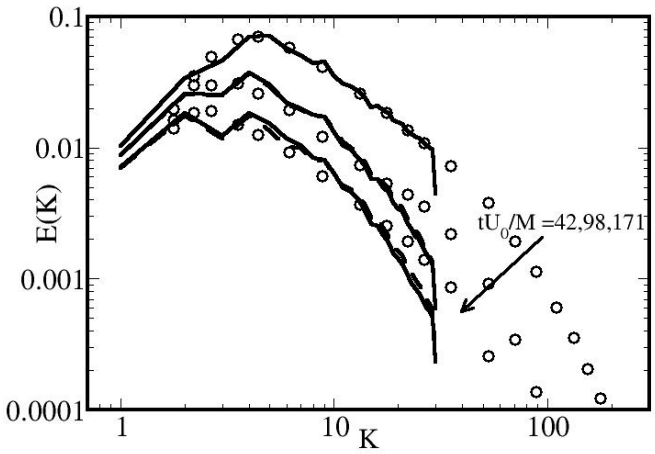

Figure 1: Three spectra at 3 times $t^* = 42, 98, 171$: ∘ Experiment of CBC; — WAD; ··· WA

prediction will not be affected since the under resolved wavelengths represent only 1% of the maximum energy. On figure 2, the spectra predicted by the dynamic Smagorinsky[4] and WALE[5] models are compared. The spectra are very similar at the different time and also in good agreement with the measurements.
The underprediction of the energy spectrum for $K > \frac{K_c}{2}$ is also observed for the dynamic Smagorinsky[4] model, supporting the fact that this issue is due to limitations of the numerical method at very high wavelengths.

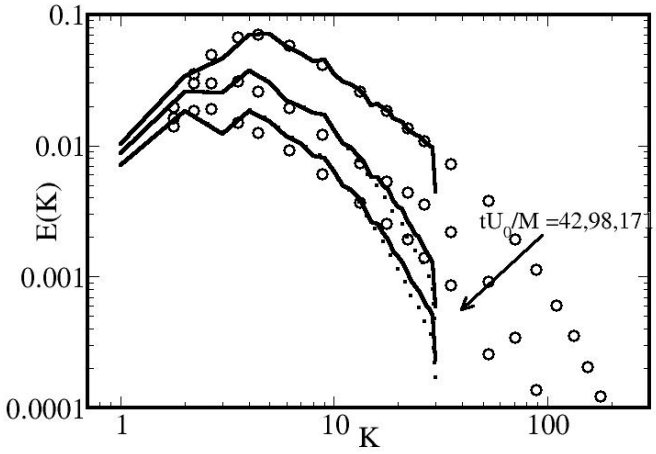

Figure 2: Three spectra at 3 times $t^* = 42, 98, 171$: ∘ Experiment of CBC; — WAD; ··· SMD

The temporal evolution of the resolved kinetic energy is also well predicted by the different models as shown in figure 3. The energy is normalised with the initial kinetic energy at time $t^* = 42$. The simulations are in good agreement with the experiment data and with the EDQNM simulations, the dynamic Smagorinsky[4] slightly underpredicts the resolved energy but still, remains in good agreement with the EDQNM results.

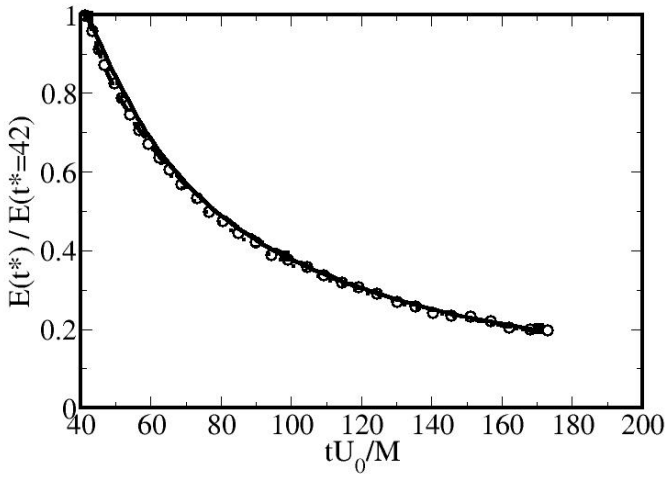

Figure 3: Temporal evolution of the resolved kinetic energy: ∘ EDQNM; — WAD; --- WA; ··· SMD

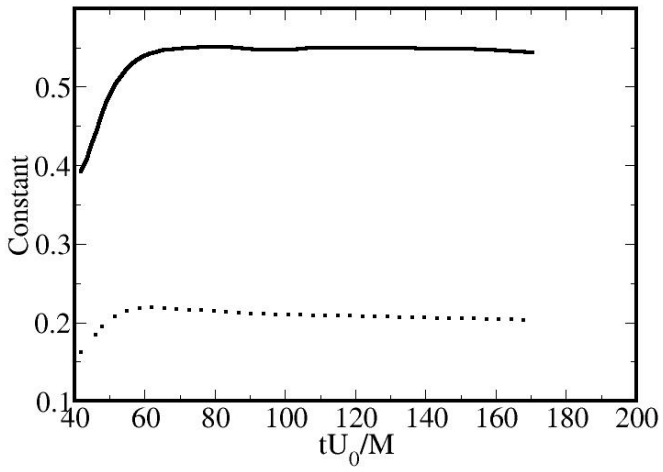

Figure 4: Temporal evolution of the dynamic constants: — WAD; ··· SMD

The temporal evolution of the dynamic constants is shown in figure 4. The dynamic

WALE constant converges to 0.55 a value closed to the one proposed by Nicoud and Ducros[5]. In the same way, the dynamic Smagorinsky constant converges to 0.2 that is closed to the canonical value, $C_s = 0.2$ performed by Clark et al.[17] for a HIT.

4 TURBULENT CHANNEL

4.1 Numerical set up

The periodic turbulent channel configuration is appropriate for testing the near wall behaviour of SGS models. It consists in a flow between two parallel planes (as shown in figure 5) which is driven by a source term imposed dynamically to reach a target bulk velocity:

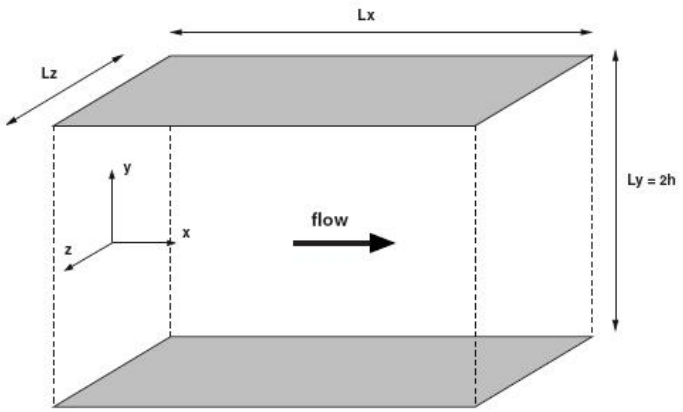

Figure 5: Turbulent channel

$$S_x = \frac{\rho U_{bulk} - \frac{1}{V}\int\int\int \rho u_x dV}{\tau_{relax}} \tag{16}$$

V is the volume of the computational domain and τ_{relax} is a relaxation time whose expression is:

$$\tau_{relax} = \frac{1}{5}\frac{h}{u_\tau}, \tag{17}$$

where u_{tau} is the friction velocity and h the channel half height. The reference data for this case are the DNS of Moser at al.[18]. The characteristics of the mesh for the friction Reynolds case $Re_\tau = 395$ are summarised in table 2. They were chosen in order to meet the requirement of the minimum turbulent channel dimensions advised by Jimenez and Moin[19].

Re_τ	$n_x \times n_y \times n_z$	$\frac{L_x}{h}$	$\frac{L_z}{h}$	Δx^+	Δz^+	Δy_w^+	Δy_c^+
395	$31 * 139 * 51$	3.5	1.3	46	10	1	17

Table 2: Characteristics of the mesh

4.2 Results

The friction Reynolds number, the friction coefficient and the error on this coefficient compared to the Petukhov[20] correlation as obtained with the different models are summarised in the table 3.

Case	$Re_\tau = 395$	C_f	% Error
WA	413	$6.55 * 10^{-3}$	9.9
SMD	396	$6.03 * 10^{-3}$	1.2
WAD	387	$5.75 * 10^{-3}$	-3.6
SVS WAD	396	$6.03 * 10^{-3}$	1.2

Table 3: Comparison of the different friction values

The main results is that the WALE model[5] over estimates the friction velocity while the dynamic WALE model slightly under estimates the friction velocity. However the dynamic Smagorinsky[4] model is in good agreement with the correlation and the expected friction velocity.

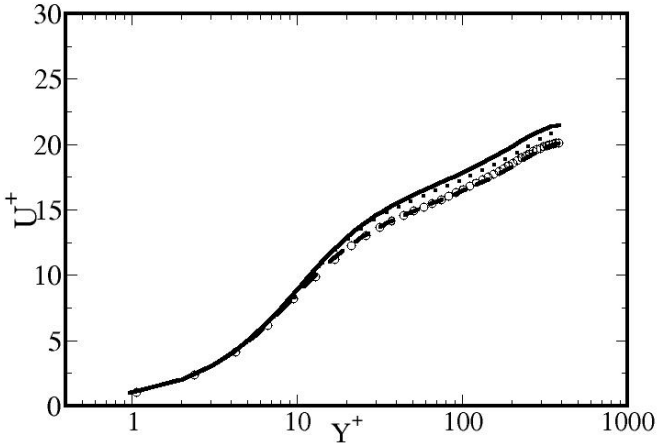

Figure 6: Mean velocity in the channel: ∘ DNS Moser et al.[18] $Re_\tau = 395$ — WAD; ··· WA; ••• SMD

Mean velocity profiles in wall units are displayed in figure 6 which shows that the dynamic Smagorinsky computation is in good agreement with the DNS data of Moser et al.[18] with a slight overprediction of the mean velocity in the buffer-layer. The dynamic

WALE model does not improve the WALE[5] model and its velocity profile is not better than the dynamic Smagorinsky[4] model. The mean velocity is clearly overestimated from the buffer-layer to the centre of the channel. This is due to the overestimation of the viscosity as depicted in figure 7 due to high value of the constant near the wall as shown in figure 8. The WALE computations are in good agreement with the DNS but it is certainly due to the overprediction of the friction veolicty as shown in table 3. Considering the eddy viscosity, figure 7 shows that the dynamic Smagorinsky model[4] does not have a y^{+3} asymptotic behaviour in contrary to what was obtained by Germano et al.[3]. This is due to the stabilisation method that is not performed over the homogeneous directions, as already mentionned in section 2.
The cubic asymptotic behaviour is better retrieved by the WALE[5] and the dynamic WALE models because they are built with the spatial operator of Eq.5. However, the eddy viscosity from WALE is substantially smaller than the values obtained by both dynamic models in the turbulent region ($y^+ > 30$). On the other hand, the dynamic WALE produces too large eddy-viscosity in the buffer-layer ($5 < y^+ < 30$). These behaviours are better understand by considering the profiles of the model constant, as depicted in figure 7. It strongly decreases in the near wall region for the dynamic Smagorinsky[4] model since the dynamic procedure is required to damp the eddy viscosity, if the Smagorinsky[1] model is used. The opposite is observed for the dynamic WALE model for which the model constant is 40 times larger than the value proposed by Nicoud and Ducros[5] (10 against 0.25). Note that even in the core region, the dynamic procedure generates a constant which is approximatively 3 times larger than its static counter part. This situation is different from what is observed for the dynamic Smagorinsky[4] model; in this case the dynamic constant (0.18^2) in the core region is close to the classical model constant as shown in figure 8.

The dynamic version of the WALE model leads to very high value of the constant near the wall and to a bad prediction of the mean velocity. It rises the question of the effectiveness of the Germano-identity when developping a dynamic version of a model that has a right asymptotic behaviour. This was already observed by Park et al.[21] in their attempt to develop a dynamic version of the Vreman's model[6] based on the Germano-identity. They observed a low correlation between the SGS tensor predicted by the dynamic model with the true SGS tensor specially near the wall. They then developed a global dynamic model improved by You and Moin[22] where a global equilibrium instead of the local equilibrium was assumed. The final constant was homogeneous in space but time dependent. The main drawback of such a global dynamic procedure is that it relies on the SGS model to ensure that the spatial variations in the eddy viscosity are properly obtained. Notably, one could expect that ν_{sgs} goes to zero with the appropriate y^{+3} behaviour near solid wall and at the same time vanishes in region of pure rotation. However, it can be easily demonstrated that the latter condition is not met for both the Vreman's[6] nor the WALE[5] models. It is then still necessary to investigate if a local version of those dynamic models can be developed. This is discussed in the next section.

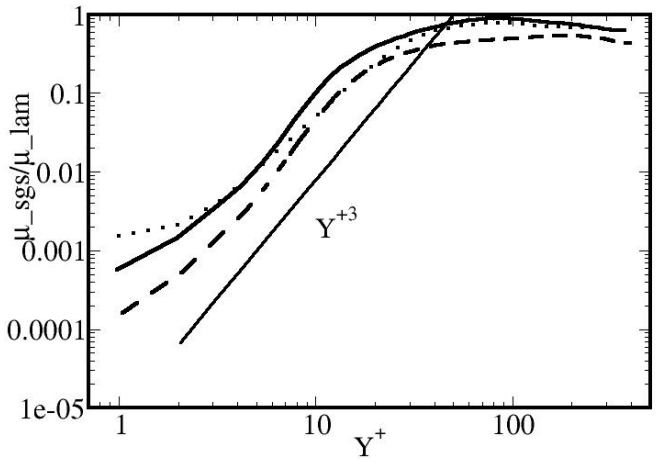

Figure 7: Mean viscosity in the channel: — WAD; --- WA; ··· SMD

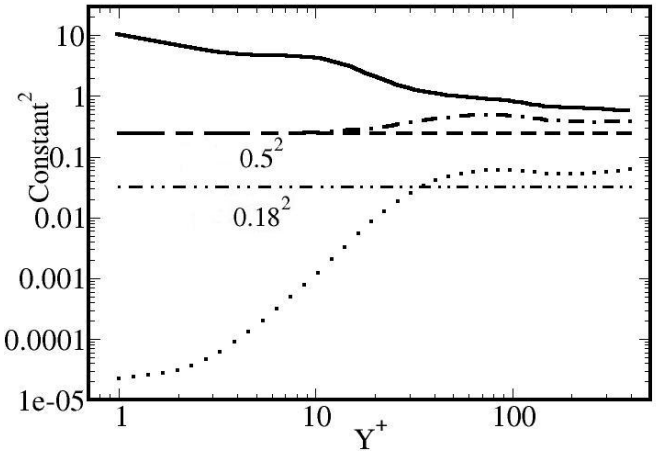

Figure 8: Square of the constant in the channel: — WAD; ··· SMD; – · – SVS WAD

5 MODIFIED DYNAMIC WALE MODEL

5.1 Theoretical study

The behaviour of the eddy viscosity and the constant in the channel shown respectively in figure 7 and 8 point out that the main problem of the model is near the wall. In fact for $Y^+ > 30$ the eddy viscosity predicted by the dynamic WALE and Smagorinsky[4] models are almost similar but the high values of the constant near the wall have an impact on

the viscosity in the buffer-layer.
In order to better understand this behaviour, we have first carried out a theoretical study of the asymptotic behaviour of the numerator and denominator of expression (11).

Considering a filtered incompressible velocity field $\bar{u}_1, \bar{u}_2, \bar{u}_3$ the asymptotic behaviour of the different components of the velocity are expressed as :

$$\begin{aligned} \bar{u}_1 &= ay + by^2 + O(y^3) \\ \bar{u}_2 &= cy^2 + O(y^3) \\ \bar{u}_3 &= dy + ey^2 + O(y^3) \end{aligned} \tag{18}$$

where a, b, c, d and e depend on x, z and time. We only consider the components that are most important near the wall. Then M_{ij}^w and L_{ij} will be simplified to M_{12}^w and L_{12} and we have the following behaviour:

$$\begin{aligned} M_{12}^w &= \hat{\Delta}^2 |\hat{\bar{O}P}| \hat{\bar{S}}_{12} - (\bar{\Delta}^2 \widehat{|\bar{O}P|} \bar{S}_{12}) \\ L_{12} &= \widehat{\bar{u}_1 \bar{u}_2} - \hat{\bar{u}}_1 \hat{\bar{u}}_2 \end{aligned} \tag{19}$$

From the expression 18, we have:

$$\begin{aligned} S_{12} &= a + O(y) \\ \bar{u}_1 \bar{u}_2 &= acy^3 + O(y^4) \end{aligned} \tag{20}$$

and the operator $|\bar{OP}|$ that is based on the WALE model[5] has a y^3 behaviour.

$$|\bar{OP}| = fy^3 + O(y^4) \tag{21}$$

With the relation Eq.20 and Eq.21 the terms L_{ij} and M_{ij} have the following behaviour:

$$\begin{aligned} M_{12}^w &= \hat{\Delta}^2 fay^3 - (\widehat{\bar{\Delta}^2 fay^3}) + O(y^4) \\ L_{12} &= \widehat{acy^3} - \widehat{ay}\widehat{cy^2} + O(y^4) \end{aligned} \tag{22}$$

Then near the wall, the dynamic constant converges to the following expression:

$$C_w = \frac{< \widehat{acy^3} - \widehat{ay}\widehat{cy^2} >}{< \hat{\Delta}^2 fay^3 - (\widehat{\bar{\Delta}^2 fay^3}) >} + O(y) \tag{23}$$

This relation shows that the dynamic constant formally behaves like y^0 near the wall. However, the leading order term in Eq.23 is the ratio of two very small quantities (behaving like y^{+3}) whose numerical assessment strongly depends on the details of the test filter application and stabilisation procedure. This situation is obviously ill-posed numerically and can lead to very large value of the dynamic constant, as observed in fig 8. Note that the situation is drastically different when the dynamic procedure is applied to the Smagorinsky[1] model. In this case, the spatial operator $|\bar{OP}|$ behaves like y^0 and the denominator of Eq.23 also. A model with a proper asymptotic behaviour seems to be more sensitive to the choice of the filters and the stabilisation, specially near the wall.

5.2 Proposed solution

The analysis conducted in section 5.1 suggests that the SGS models that have the correct behaviour near the wall could be very sensitive to the filtering procedure and the stabilisation method. This could be a real drawback to the development of any dynamic version based on the Germano-identity for those models. Since the laminar viscosity is dominant in the vicinity of the wall, there is no need, if one considers a SGS model with the proper wall behaviour, to adapt its constant dynamically in the near wall region. Still, it remains necessary to evaluate the constant in fully developed turbulent parts of the flow.
A simple way to achieve this is to identify the "near wall region". In other words, to have a sensor able to detect the presence of the wall without a priori knowledge of the geometry which can be arbitrary complex. Such a sensor is not unique. Here we propose to make use of an invariant similar to the one involved in the WALE model[5] (see Eq.5) More precisely, we have selected the following dimensionless parameter:

$$SVS = \frac{(S^d_{ij}S^d_{ij})^{3/2}}{(S^d_{ij}S^d_{ij})^{3/2} + (S_{ij}S_{ij})^3} \tag{24}$$

which has the following properties :

- the SVS behaves like y^{+3} since it shares the same numerator than the WALE operator (Eq.5),
- the $SVS = 0$ for pure shear flows for the same reason,
- the $SVS = 1$ for pure rotating flows since $S_{ij} = 0$ in this case

This last property indicates that SVS is bounded by $0-1$, its lower value corresponding to pure shear flows, its larger value corresponding to pure rotating flows. This also justifies the acronym SVS (Shear and Vortex Sensor) we have chosen for this sensor.

Figure 9 shows the SVS in the channel as a function of y^+ for the $Re_\tau = 395$.

It illustrates that this quantity can be used to divide the simulated geometry into two zones: a zone far from the wall where the model constant should be estimated dynamically using the Germano-identity and a zone close to the wall where the constant should be fixed to 0.5, suggested by Nicoud and Ducros[5]. The value 0.09 is considered here as the value below which the SVS behaves nearly y^{+3} and was thus chosen as threshold value (see figure 9).
The modified dynamic WALE model is then expressed as follows:
if $SVS > 0.09$

$$C^2_{wsvs} = \frac{1}{2}\frac{< L_{ij}M^w_{ij} >^+}{< M^w_{ij}M^w_{ij} >} \tag{25}$$

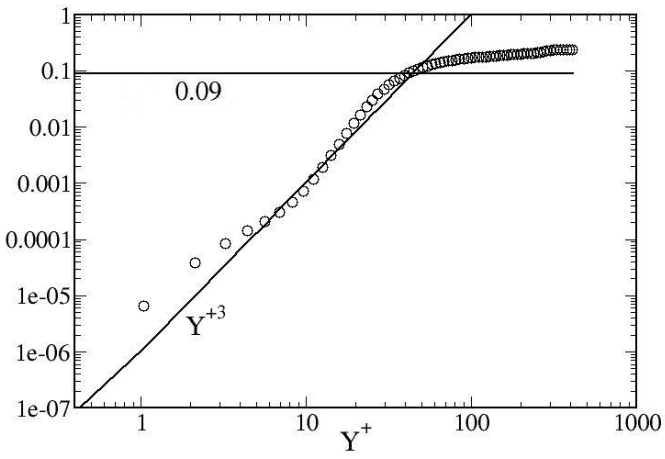

Figure 9: SVS in the channel at $Re_\tau = 395$

and if $SVS < 0.09$

$$C^2_{wsvs} = 0.25 \tag{26}$$

5.3 Results of the dynamic WALE with SVS at $Re_\tau = 395$

The modified model has been validated on the HIT of Comte-Bellot and Corsin[7] and the results are similar to those obtained with the normal dynamic WALE model. We will then only focus on results obtained in the turbulent channel.
Results of the friction value obtained with the SVS dynamic WALE (see table 3) show that the model has improved the prediction of the the static WALE model[5] and are similar to those obtained with the dynamic Smagorinsky model[4].

Figure 10 compares the mean velocity predicted by the modified dynamic WALE, the dynamic Smagorinsky[4] and the WALE[5] models. The mean velocity obtained with SVS dynamic WALE is in good agreement with the experiment. Figure 11 indicates that the viscosity in the channel is no longer affected by the high values near the wall. This is also illustrated in fig 8.

The figure 8 compared the prediction of the square of the dynamic WALE constant obtained with the normal and the modified dynamic WALE model. The introduction of the SVS helps to controlling the value of the constant near the wall while keeping the dynamic computation of the constant in the core region of the channel. This combination leads to a better results than the WALE model[5].

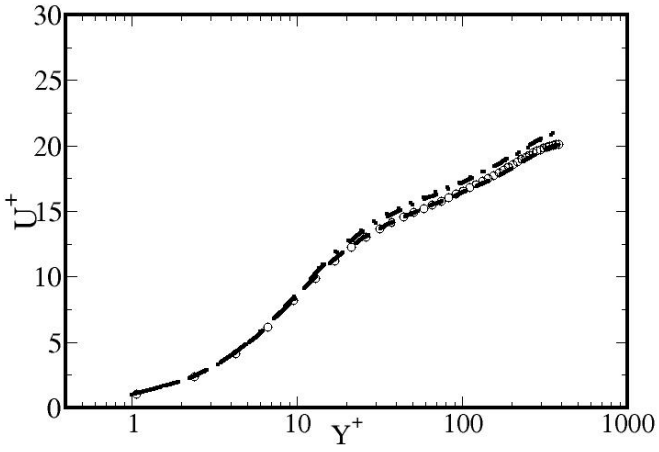

Figure 10: Mean velocity in the channel at $Re_\tau = 395$: ∘ DNS Moser et al.[17] $Re_\tau = 395$; ··· SMD; – · – SVS WAD

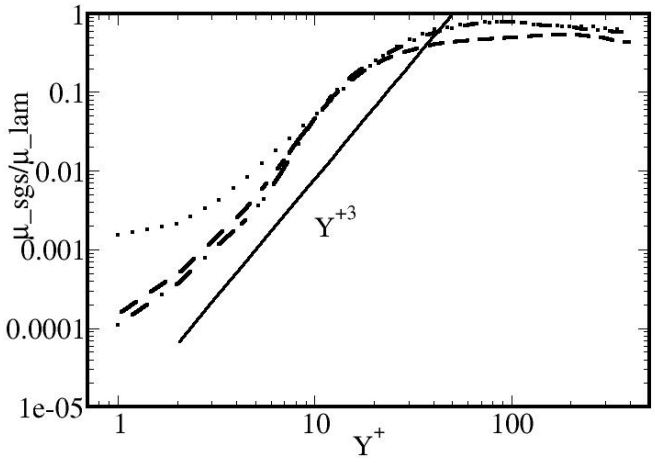

Figure 11: Eddy viscosity in the channel at $Re_\tau = 395$: ··· SMD; – · – SVS WAD

5.4 Results of the dynamic WALE with SVS at $Re_\tau = 590$

In an attempt to assess the adaptability of the procedure, we have kept the same mesh to compute the $Re_\tau = 590$ channel flow, also computed by Moser et al.[18] The characteristics of the mesh in wall units are summarised in the table 4.

Re_τ	$n_x \times n_y \times n_z$	$\frac{L_x}{h}$	$\frac{L_z}{h}$	Δx^+	Δz^+	Δy_w^+	Δy_c^+
590	$31 * 139 * 51$	3.5	1.3	65	14	1.4	24

Table 4: Characteristics of the mesh for the case $Re_\tau = 590$

Figure 12 shows the mean velocity in channel obtained with the modified dynamic WALE model. The velocity is slightly overestimated in the centre of the channel probably due to the resolution but results are still in good agreement with the DNS.

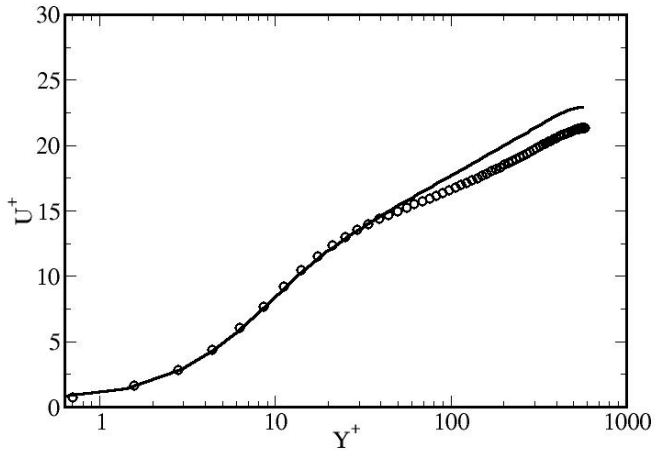

Figure 12: Mean velocity in the channel at $Re_\tau = 590$: ∘ DNS Moser et al.[17] ; — SVS WAD

Figure 13 shows the rms velocity. Although the maximum of the axial velocity is overestimated, the location of the maximum is reasonably well predicted by the simulations. The poor resolution of the mesh in the streamwise and spanwise directions is certainly the main cause of the discrepancies observed in figure 13.

The eddy viscosity is represented in figure 14. Even at this high wall Reynolds number the near wall behaviour of the model is preserved.

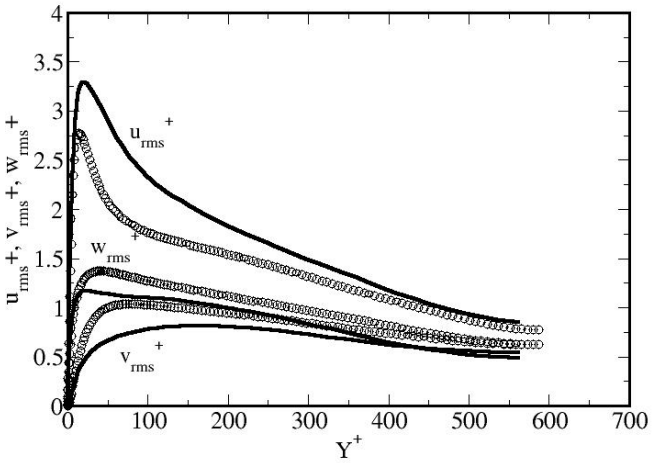

Figure 13: Root mean square of velocity in the channel at $Re_\tau = 590$: ∘ DNS Moser et al.[18]; — SVS WAD

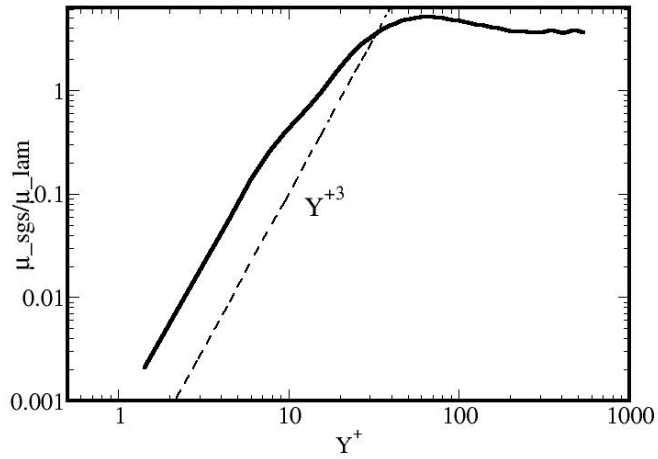

Figure 14: Sgs viscosity in the channel at $Re_\tau = 590$

The dynamic constants of the SVS WALE model are represented in figure 15 for the two friction Reynolds numbers. The constants clearly adapt their value to the flow in the turbulent part of the channel while the SVS keeps the same behavior (see figure 16). The only difference is due to the y^+ resolution that increased from the low to the high friction Reynolds number case when using the same mesh.

It is worth nothing that even by adding high level of artificial viscosity during the

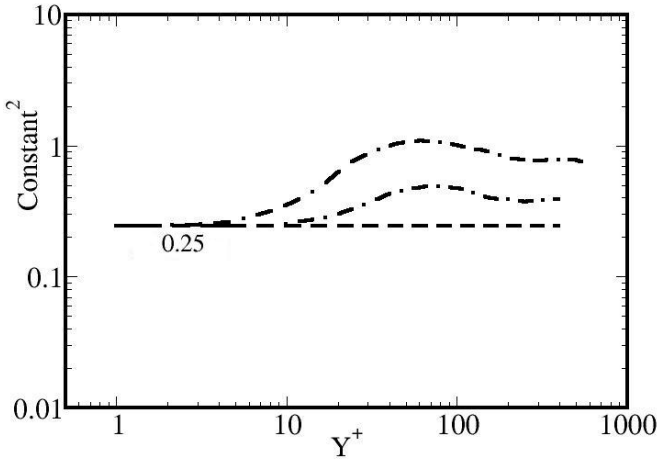

Figure 15: Constants of the SVS WAD for the two friction Reynolds number: $- \cdot - Re_\tau = 395$; $\cdot - - Re_\tau = 590$

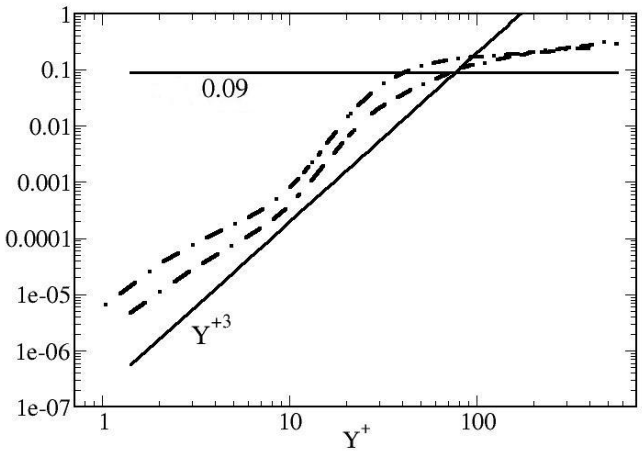

Figure 16: SVS for the two friction Reynolds number: $- \cdot - Re_\tau = 395$; $\cdot - - Re_\tau = 590$

runs, no satisfying results were obtained with the dynamic Smagorinsky model[4]. This is probably due to the fact that no averaging on homogeneous directions as discussed in section 2. This indicates that the SVS dynamic WALE model has greater potential than the dynamic Smagorinsky model[4] for complex/high Reynolds configurations while leading to equivalent results in simple/moderate Reynolds situations.

6 CONCLUSIONS

A dynamic version of the WALE model[5] with a Shear and Vortex Sensor has been proposed. The model was succefully implemented and tested on the HIT experiment of CBC[7]. The model gives equivalent results than the dynamic Smagorinsky model[4] at low friction Reynolds number and better results at high Reynolds number in an isothermal turbulent channel configuation. In contrary to the dynamic Smagorinsky constant, the dynamic WALE constant does not need to be averaged over homogeneous direction and is then more suitable for very complex flows and geometries. In order to avoid highest values of the viscosity in the laminar zone of the boundary layer due to the use of the Germano-identity and the small value of the WALE operator near the wall, the SVS has been introduced to divide the flow in two regions. A first one, close to the wall where the constant keeps the value advised by Nicoud and Ducros[5] and a second one corresponding to the fully developped parts of the flow where the constant is dynamically evaluated and can adapt to the mesh resolution and the turbulent flow level. The resulting viscosity still has the proper y^{+3} behavior near the wall. The SVS dynamic WALE model seems promising for modelling turbulent flow in very complex geometries without important additional CPU cost and control strategies with equivalent or even better results than the dynamic Smagorinsky model[4] and static constant SGS models.

REFERENCES

[1] J. S. Smagorinsky, General circulation experiments with the primitive equations, *Mon. Weather Rev.*, **Vol. 91**, 99-164 (1963).

[2] P. Sagaut, Large eddy simulation for Incompressible flows, *Springer-Verlag Berlin and Heidelberg GmbH & Co. K*, (1998).

[3] P. Moin and J. Kim, Numerical investigation of turbulent channel flow, *J. Fluid Mech.* , **Vol. 118**, 341-377 (1982).

[4] M. Germano, U. Piomelli , P. Moin,W. H. Cabot, A Dynamic Subgrid-Scale Eddy Viscosity Model, *Physics of Fluids*, **No. A3**, 1760-1765 (1991).

[5] F. Nicoud, F. Ducros, Subgrid-scale stress modelling based on the square of the velocity gradient tensor, *Flow, Turbulence and Combustion*, **Vol. 62** 183-200 (1999).

[6] A. W. Vreman , An eddy-viscosity subgrid-scale model for turbulent shear flow: Algebraic theory and applications, *Physics of Fluids*, **Vol. 16 No. 3**, 3670 (2004).

[7] G. Comte-Bellot, S. Corrsin, Simple Eulerian time correlation of full- and narrow-band velocity signals in grid generated, isotropic turbulence, *J. Fluid Mech.* **Vol. 48**, pp.273-337 (1971).

[8] D. K. Lilly, A proposed modification of the Germano subgrid scale closure model, *Physics of Fluid*, **A 4** (633).

[9] G. Ghorbaniasl and C. Lacor., Sensitivity of sgs models and of quality of les to grid irregularity, *In J. Meyers et al. (Eds), Quality and Reliability of Large-Eddy Simulations. Springer Science + Business Media B.V.* (2008).

[10] V. Moreau, G. Lartigue, Y. Sommerer, C. Angelberger, O. Colin and T. Poinsot, High order methods for DNS and LES of compressible multicomponent reacting flows on fixed and moving grids S. *J. Comp.Phys.* **Vol. 202 (2)**, pp.710-736 (2005).

[11] O. Colin and M. Rudgyard, Development of high-order Taylor-Galerkin schemes for unsteady calculations, *J. Comput. Phys.*, **162**, 338 (2000).

[12] O. Cabrit and F. Nicoud, Direct simulations for wall modeling of multicomponent reacting compressible turbulent flows, *Physics of Fluids*, **21**, (2009).

[13] A. Scotti, C. Meneveau, A fractal model for large eddy simulation of turbulent flow *Physica D* **127**, (1998).

[14] N. Park, K. Mahesh, A velocity-estimation subgrid model constrained by subgrid scale dissipation *J. Comp. Phys.*, **227**, 4190-4206, (2008).

[15] N. Park, K. Mahesh, Reduction of the Germano-identity error in the dynamic Smagorinsky model, *Physics of fluids*, **21**, (2009).

[16] N. Park, K. Mahesh, Analysis of numerical errors in large eddy-simulation using sattistical closure theory, *J. Comp. Phys.*, **222**, (2007).

[17] R. A. Clark, J. H. Ferziger, W.C.A. Reynolds, Evaluation of subgrid-scale models using an accurately simulated turbulent flow, *Journal of Fluid Mechanic*, **91(1)**, (1979).

[18] R. D. Moser, J. Kim and N. N., Direct numerical simulation of turbulent channel flow up to $Re_\tau = 590$, *Physics of Fluids*, **Vol. 11, No. 4**, pp. 943-945 (1999).

[19] Jiménez and P. Moin, The minimal flow unit in near-wall turbulence, *J. Fluid Mech*, **225** (1991).

[20] M. W. Kays, M. E. Crawford and B. Weigand, B. Convective Heat and Mass Transfer, Fourth Edition, *McGraw-Hill International Edition* .

[21] N. Park, S. Lee, J. Lee, and H. Choi. A dynamic subgrid-scale eddy viscosity model with a global model coefficient. *Physics of Fluids*, **18**, (2006).

[22] D. You and P. Moin. A dynamic global-coefficient subgrid-scale eddy-viscosity model for large-eddy simulation in complex geometries. *Physics of Fluids*, **19** (2007).